Nonradiative Excitation Energy Transfer in Hydrophobically Modified Amphiphilic Block Copolymer Micelles. Theoretical Model and Monte Carlo Simulations†,‡

Filip Uhlík, Zuzana Limpouchová, Pavel Matějíček, and Karel Procházka*

Department of Physical and Macromolecular Chemistry & Laboratory of Specialty Polymers, School of Science, Charles University in Prague, Albertov 6, 128 43 Prague 2, Czech Republic

Zdeněk Tuzar

Institute of Macromolecular Chemistry, Czech Academy of Sciences, Heyrovský Square 2, 162 06 Prague 6, Czech Republic

Stephen E. Webber

Department of Chemistry and Biochemistry, University of Texas at Austin, Austin, Texas 78712

Received November 28, 2001; Revised Manuscript Received July 30, 2002

ABSTRACT: A general approach for analyzing the direct nonradiative excitation transfer from donors to traps (NRET) in systems of specifically tagged polymeric micelles is presented. We assume that the micelles are formed by a hydrophobic/hydrophilic diblock copolymer in a strongly polar selective solvent. The micelle-forming chain is tagged by a donor between blocks and by a strongly hydrophobic trap at the end of the hydrophilic shell-forming block. When micelles are formed the donors are trapped at the core/shell interface and the hydrophobic traps try to avoid the polar medium and return back into the shell. Formation of compact chain conformations or loops is entropically unfavorable and the spatial distribution of traps in the shell is a result of the enthalpy-to-entropy interplay. Several physically reasonable but simplified models for the distributions of traps in the shell have been studied in detail. Representative results of computer-based Monte Carlo simulations of the time-resolved donor fluorescence decay as affected by NRET are presented for these systems. Comparison of our calculated and experimental curves allows us to evaluate the distribution of traps in micellar shells of double-tagged micelles.

Introduction

Fluorescence techniques have proved to be a very useful tool for studying conformations of macromolecules and various processes in biochemistry and polymer science.[1−4] Nonradiative excitation energy transfer (NRET) has been widely used in studies of polymer compatibility, concentration correlation and conformational changes.[5−12] Several authors have also applied NRET for the investigation of polymeric micelles, which is the subject of this paper.[13−19]

Polymeric micelles are spherical nanoparticles containing a compact insoluble core (formed by blocks B) and a protective shell (formed by blocks A). They form spontaneously upon dissolution of a hydrophobic/hydrophobic block copolymer AB in a selective solvent (good solvent for block A and nonsolvent for block B).[20] Hydrophobic/hydrophilic block polyelectrolytes also form micellelike nanoparticles in aqueous media.[21−36] However, the polymers are often insoluble in water and micelles have to be prepared initially in an aqueous/organic mixed solvent and transferred into aqueous buffers by dialysis.[37,38]

We have been studying the micellization of high-molar-mass block copolymers and polyelectrolytes for a long time, both experimentally and theoretically.[37−47] In this paper, we present a Monte Carlo (MC) approach for the interpretation of NRET data in solutions of polymeric micelles with fluorophores attached at specific parts of the copolymer chains. Specifically the fluorescent energy donor (naphthalene) is a pendant group in the bridge connecting the hydrophobic (polystyrene) and hydrophilic (poly(methacrylic acid)) blocks and the fluorescent energy acceptor (anthracene) is attached at the end of the hydrophilic block (Chart 1). The results of our computer simulations will be compared to the experimental data presented in the preceding paper.[48]

NRET in Specifically Tagged Micellar Systems

The correct analysis of time-resolved fluorometric data for a polymeric system containing a large number of identical energy donors, N_D, and a comparable number of traps, N_T, is complex and requires knowledge of the distribution function of donor-to-trap distances, $w_{DT}(r)$. For a particular configuration of N_T fixed traps around a donor that was excited at $t = 0$ the probability, $\rho(t)$, that the donor is still excited at t is given by the following master equation[49]

$$\frac{d\rho}{dt} = -\left[\frac{1}{\tau_D} + \sum_{i=1}^{N_T} k_{tr}(r_i)\right]\rho \qquad (1)$$

* To whom correspondence should be sent. E-mail: prochaz@vivien.natur.cuni.cz.

† The study is a part of the long-term research plan of the School of Science, Charles University in Prague, No. MSM 113100001.

‡ Dedication. The authors would like to dedicate the paper to Prof. Petr Munk, Professor Emeritus from the University of Texas at Austin at the occasion of his 70th birthday.

10.1021/ma012073o CCC: $22.00
Published on Web 10/29/2002

Chart 1

PS–N–PMA–A

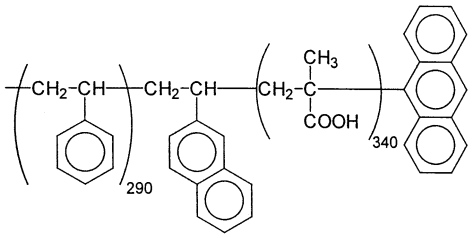

PS–N–PMA

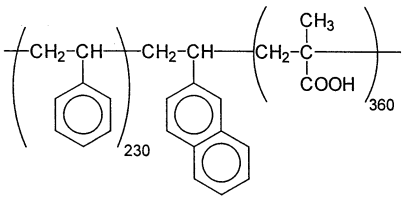

where τ_D is the fluorescence lifetime of the donor in a given medium (unaffected by NRET to traps) and $k_{tr}(r_i)$ are the transfer rate constants depending on the donor-to-trap distances, r_i. If the energy transfer occurs via the Förster dipole−dipole exchange mechanism[50,51] then $k_{tr}(r) = (1/\tau_D)(R_0/r)$,[6] where R_0 is the Förster radius, for which $k_{tr}(R_0) = 1/\tau_D$. The solution of eq 1 yields the survival probability $\rho(t)$ for a given fixed configuration of traps with respect to one randomly excited donor. If the separations of the donor groups are significantly larger than the Förster radius for donor−donor energy transfer, energy migration among donors does not have to be taken into account. For the case of naphthalene donors on the micelle core−corona interface in our experimental system, this assumption is justified. Calculation of their average separation based on the structural characteristics of PS−N-PMA-A micelles leads to a value ca. 3.2 nm. The value of R_0 for naphthalene self-transfer is small (e.g., naphthalene, 0.76 nm; 1-methylnaphthalene, 0.83 nm; 2-methylnaphthalene, 0.86 nm).[52] In our earlier studies with 9,10-diphenyl-anthracene (DPA) tagged micelles, PS-DPA-PMA, with essentially the same number of tags per micelle and core radius, we have found very high fluorescence anisotropy.[53] This finding indicated that the donor groups were unable to rotate in the dense medium and also that the donor−donor energy migration was negligible because either of these processes would have depolarized the fluorescence. Naphthalene has a fairly long fluorescence lifetime, and it is not a good probe for anisotropy studies. Nevertheless, we have measured the naphthalene steady-state anisotropy and obtained a value of 0.25 for micelles in water, rather high for a long-lived probe. Certainly this implies an absence of either rotation of the naphthalene or energy transfer between naphthalene moieties.

Each specific positioning of a set of traps species on the "lattice" that surrounds the donor corresponds to a particular exponential decay for the donor and the observed fluorescence decay is an average over all the possible position of the traps. Let us assume a system of N_T traps that may be located in N_L "lattice sites". If both the positions of the trap species and the number of trap species in each lattice site, n_i, can fluctuate, then one can write

$$I_D^q(t) = I_0 \exp(-t/\tau_D)\prod_{r_j=0}^{N_L}\sum_{n_j=0}^{N_T} g(r_j,n_j)[\exp(-k(r_j)t)]^{n_j} \quad (2)$$

where $k(r_j)$ is the same as $k_{tr}(r)$ given above (r_j is the donor and trap separation for the jth lattice site, n_j is the number of traps on the jth lattice site, and $g(r_j,n_j)$ is the probability that there are n_j traps on the jth latice site). $I_D^q(t)$ is the fluorescence intensity, which is proportional to the product of the average $\rho(t)$ value (from eq 1) and the quantum yield of fluorescence and I_0 is the fluorescence intensity at $t = 0$. If $g(r_j,n_j)$ is given by the Poisson distribution function, i.e., $g(r_j,n_j) = (\langle n_j\rangle^{n_j}/n_j!)\exp(-\langle n_j\rangle)$ then the Klafter and Blumen[54] (KB) equation is obtained:

$$I_D^q(t) = I_0 \exp(-t/\tau_D)\exp\left\{-\rho_T\int_0^\infty [1 - \exp(-k(r)t)]w_{DT}(r)\mathrm{d}V\right\} \quad (3)$$

where ρ_T is the average density of traps and $w_{DT}(r)$ is the dimensionless distribution of donor−trap distances.

This equation has been widely discussed (Klafter and Blumen,[54,55] El-Sayed,[56,57] Fayer and co-workers,[58−62] Frederickson and Frank[63,64]). Following the Klafter−Blumen formalism,[54] Winnik and co-workers derived formulas describing energy transfer in restricted systems with spherical symmetry.[65,67] While these formulas look very attractive for the treatment of experimental decays in the double-tagged micellar systems described here, the KB equation is only valid for low densities of traps that are independently placed on the lattice (this is implicit in the use of the Poisson distribution). This is not necessarily the case in our system of interest, as each donor has one acceptor directly bonded to the same polymer chain and other acceptors bonded to different chains. Because the local density of shell-forming coils near the core−shell interface is high, excluded volume considerations are important which can lead to strong correlations between the location of the trap species.

To illustrate the above comments, we consider a "simplistic" model with a constant surface density of traps at distance R_T from the micellar center (i.e., we assume that all trap-tagged ends of the shell-forming blocks return back to the same distance from the micellar center and that the traps are homogeneously distributed on a spherical surface of radius R_T with a constant surface density, $\rho = N_T/(4\pi R_T^2)$). Therefore, each donor sees exactly the same distribution of traps, and therefore, the fluorescence decay is a single exponential. The energy transfer rate constant is given by

$$(k_{tr})_{mean} = \left(\frac{1}{\tau_D}\right)N_T R_0^6\int_{R_T-R_C}^{R_T+R_C}\frac{P(r)}{r^6}\mathrm{d}r = \frac{R_0^6 N_T}{\tau_D}\frac{R_T^2 + R_C^2}{(R_T^2 - R_C^2)^4} \quad (4)$$

where function $P(r)$ describes the normalized number density of traps in the distance r from the excited donor. This function may be obtained in the analytical form, $P(r) = r/(2R_CR_T)$ (see Appendix 1).

In this simple model system, the transfer efficiency, χ^{tr}, is given by the following formula

$$\chi^{tr} = \frac{R_0^6 \int_{R_T-R_C}^{R_T+R_C} \frac{P(r)}{r^6} dr}{R_0^6 \int_{R_T-R_C}^{R_T+R_C} \frac{P(r)}{r^6} dr + \frac{1}{N_T}} = \frac{R_T^2 + R_C^2}{R_T^2 + R_C^2 + \frac{(R_T^2 - R_C^2)^4}{R_0^6 N_T}} \quad (5)$$

We are not aware of an application of the KB equation to this specific case of energy transfer from an inner spherical surface to a homogeneous distribution of traps on an outer spherical surface. Baumann and Fayer (BF) considered a closely related model system in which a donor confined to one surface transfers energy to traps on another plane located at distance d.[68] The overall analysis is complicated and these workers find two limiting cases depending on the value of the parameter $\mu = (3/2)(t/\tau_D)(R_0/d)^6$. For $\mu < 0.05$ (small time or large d) the donor decay is exponential:

$$\ln\langle I_D(t)\rangle = -t/\tau_D - (\rho\pi/2)(R_0^6/d^4)(t/\tau_D) \quad (6)$$

If we use the identity $(R_T^2 - R_C^2)^4 = (R_T - R_C)^4(R_T + R_C)^4$ in expression 5 above and assume that both R_T and R_C are sufficiently large compared to their difference (i.e., $(R_T + R_C)^4 \cong (2R_T^4)$, we recover eq 6 exactly. It is to be expected that concentric spheres in the limit of large radii are equivalent to parallel surfaces.

BF also obtain the behavior of the donor decay for the case $\mu > 500$ (long time or small d):

$$\ln\langle I_D(t)\rangle = -t/\tau_D - (\rho\pi)(R_0^2)(3/2)^{1/3}(t/\tau_D)^{1/3} + \text{constant} \quad (7)$$

Therefore, as expected, application of the KB formalism to this model system does not produce a rigorously single exponential fluorescence decay for the donor, because this formalism implicitly assumes that the traps are distributed randomly on the second surface. For small d the fluctuations in acceptor positions are important, which lead to appreciable deviations from the single-exponential decay (our simplistic model that leads to eq 5 does not permit these fluctuations). However BF also point out that in order to apply the KB formalism the density of energy traps cannot be too high (see their eq 3.23b). In the system of our interest there may be conformations of the shell chains that yield a local density of traps that exceeds the valid range for the use of the KB formalism, especially in water-rich solvents where the shell-forming blocks loop back toward the core−shell interface frequently.

We believe that this simple model illustrates the difficulties that can occur in the application of the KB formalism to systems of our interest where the traps are not necessarily dilute or independent. Therefore, we formulate the problem from the beginning as a computer-based Monte Carlo simulation for the purpose of analyzing fluorescence decays in double-tagged micellar systems.

The Model

In this paper, we describe several simplified models for NRET which may be considered as a starting place for a more realistic description. In the following the results of Monte Carlo simulations for a hydrophobically modified convex polymeric brush will be presented and will used as a basis for the analysis of experimental decay curves presented in the preceeding paper.[48] The assumptions common to all models are based on the structural characteristics of real micellar systems and are as follows.

Scheme 1: Part of the Hydrophobically Modified (Double Tagged) Block Copolymer Micelle

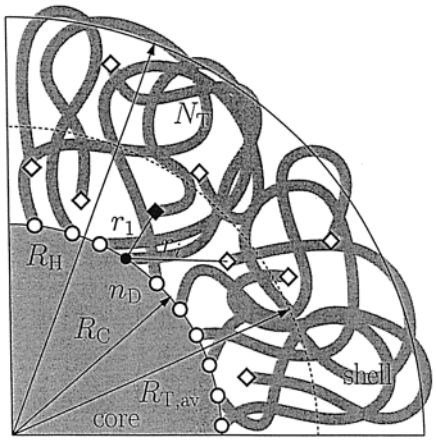

(i) Micelles are monodisperse and spherical. They contain compact spherical cores of the radius R_C. The hydrophobic core-forming and the hydrophilic shell-forming blocks are strongly segregated. The donors are chemically attached to a bridge connecting the blocks. Each micelle-forming copolymer chain contains one interblock pendant donor and one trap at the end of the hydrophilic block. We assume that all donors are distributed homogeneously along the narrow and spherical interfacial core/shell region.

(ii) The hydrophobic traps that are attached at the ends of the hydrophilic blocks try to avoid the aqueous medium, and the probability is high that they return to the inner shell, i.e., toward the core.[48] Their distribution in the shell is a result of the enthalpy-to-entropy interplay.

(iii) Under the usual experimental conditions used in fluorescence studies no more than one donor per micelle is excited. Because of the spherical symmetry of the system, all donors excited in different micelles are statistically equivalent (from the point of view of the ensemble averaging). Because the micellar solution is very dilute we consider intramicellar NRET only. We assume that the donors are immobilized in the interfacial region. According to structural characteristics of PS−N-PMA-A micelles studied experimentally, we assume that distances between donors at the interface exceed the donor−donor Förster distance and that we may neglect energy migration and excimer formation. As already mentioned this assumption is justified by our experimental studies not only on this system, but also on systems with chemically different tags (e.g., 9,-10-diphenylanthracene).[69−71]

(iv) The distribution of donor−trap separations reflects both intra- and intercoil conformations (see Scheme 1).

In the general case traps are not distributed homogeneously from the core/shell interface. Therefore, the sets of donor-to-traps distances, r_i, are neither fixed nor identical in all micelles−in other words, distances r_i fluctuate in different micelles and have to be described by distribution functions, $w_{DT}(r_i)$.

In the computer study, we generate a high number of individual sets of N_T traps in the shell by Monte Carlo simulation technique, using a priori probabilities according to the different model assumptions (described later) and calculate the normalized fluorescence decays, $I_D^q(t)/I_0$, and transfer efficiencies, χ^{tr}, for each configuration using the generic averaging formulas

$$I_D^q(t)/I_0 = \left\langle \exp\left\{-\frac{t}{\tau_D}\right\} \prod_{i=1}^{N_T} \exp\left\{-\left[\frac{R_0}{r_i}\right]^6 \left[\frac{t}{\tau_D}\right]\right\} \right\rangle_M \quad (8)$$

$$\chi^{tr} = \left\langle \frac{\dfrac{{R_0}^6}{\tau_D} \displaystyle\sum_{i=1}^{N_T} \frac{1}{{r_i}^6}}{\dfrac{{R_0}^6}{\tau_D} \displaystyle\sum_{i=1}^{N_T} \frac{1}{{r_i}^6} + \frac{1}{\tau_D}} \right\rangle_M \quad (9)$$

where $\langle\ \rangle_M$ means the averaging over the ensemble of micelles using an appropriate distribution function of donor-to-trap distances according to the considered model and I_0 is the fluorescence intensity at $t = 0$. An ensemble of 4×10^5 spherical layers with the inner radius R_C and the outer radius R_{max} was created for each model, where R_{max} is the maximum trap to micellar center distance. It is assumed that the donor lifetime is the same for all donors, we will present our results as the ratio $I_D^q(t)/I_D^0(t)$ (i.e., canceling out the trivial $\exp(-t/\tau_D)$ factor).

(a) Random Distribution of Traps in the Shell (3D Random Model). In the limit of the fully relaxed shell, we assume that the distribution of traps is fully random in the spherical layer of the thickness $\Delta R_S = R_H - R_C$, where R_H represents the hydrodynamic radius of micelles. Since the contour length of the shell-forming blocks is considerably longer than ΔR_S, the fully random distribution is quite probable in micellar systems and the corresponding behavior has to be studied. This model is very similar to one of the models discussed by Winnik et al.,[67] but it is very easy to perform the simulation and it is convenient to have curves for the same structural parameters as those for the models to be discussed below. We have performed a series of simulations for a fairly broad range of R_H values to get information how the shell swelling affects NRET in the case of a fully random (uniform) distribution of traps. Because we have found that 3D-model does not describe our micellar system well (see Results and Discussion), we do not go into detail comparing our data with analytical decays by Winnik.

(b) Gaussian Distribution of Traps in the Shell. The second model of the shell with fluctuating traps reflects the fact that the end-attached traps prefer the nonpolar medium and try to bury themselves in the inner shell, but they are pulled toward the shell periphery by the shell-forming chains. Because of the enthalpy-to-entropy interplay, we assume that a certain distance R^{ef}, from the core/shell interface provides the most favorable thermodynamic conditions for the location of traps. Therefore, we assume that positions of traps fluctuate in the radial direction with a probability density $\varphi(r)$ that has a maximum at R^{ef}. For simplicity, we use the Gaussian function, $\varphi(r) = A \exp[-(r - R^{ef})^2/(2\sigma_T^2)]$ (A is the normalization constant and the standard deviation is described by σ_T). Because of the spherical symmetry of micelles, the angular distribution of traps is fully random.

In the limit of $\sigma_T = 0$, the model describes a system of "pseudo-uniform" micelles, and all traps return to the same distance from the micellar center (similar to the simplistic model discussed earlier).

(c) Maxwellian Distribution of Traps. The last model we consider reflects the brush characteristics of the shell more realistically than the Gaussian model. Similarly to the previous one, we assume that the angular distribution of traps is uniform.

The micellar shell may be treated as a brush on a spherical surface. This system has been already studied using various methods.[72−75] The free ends density for a brush of simple polymer chains on a spherical surface was treated by Wijmans and Zhulina,[73] but their results cannot be directly applied to our case of chains with attached hydrophobic traps. We assume that the trap density is proportional both to the free volume (filled-in by solvent molecules) and to the Boltzmann factor. Both factors may be estimated from the segment density. It has been found that for brushes grafted onto moderately curved spherical surfaces the segment density is parabolic, just like a flat surface.[75]

$$\Phi(z) = \Phi(R_C)(1 - (z/R_H)^2) \quad (10)$$

where $z = r - R_C$ is the distance from core/shell interface and R_H is the hydrodynamic radius (taken to be the maximum extension of the corona).

In our case, we decided to use the parabolic profile as the first approximation. Under this assumption the free volume in the distance r from the micellar center is proportional to $\Phi(R_C)(r - R_C)^2/R_H^2$ and the potential energy of a trap, W_T (which depends on interactions with segments, E_{TP} and solvent molecules, E_{TS}) is $W = \Phi(R_C)(r - R_C)^2 E_{TS}/R_H^2$, provided that the reference trap−polymer segment interaction energy, E_{TP}, has been set to zero. Then the trap density $\varphi(r)$ may be expressed as

$$\varphi(r) = A(r - R_C)^2 \exp[-(r - R_C)^2/(2\sigma^2)] \quad (11)$$

where the normalization factor $A = 2/(\sqrt{2\pi}\ \sigma^3)$, the quantity σ is proportional to both temperature and hydrodynamical radius R_H and inversely proportional to interaction energy E_{TS}. The trap density $\phi(r)$ is a Maxwellian density with mean $\langle r \rangle = R_C + 2\sigma\sqrt{2/\pi}$, standard deviation $\sqrt{3-8/\pi}\ \sigma$ and mode $R_C + \sqrt{2}\ \sigma$.

Results and Discussion

Examples of MC Calculations. The proposed approach is fairly general and may be used for any model for the distribution function of traps in the hydrophobically modified micelle and for any number of traps N_T. The only practical limitation is that the distribution of traps has to decay sufficiently rapidly in the radial direction.

Our model polymeric micelles discussed here will have structural characteristics appropriate to our experimental study of polystyrene-*block*-poly(methacrylic acid) micelles in highly polar solvents. The polymers that make up these micelles are doubly tagged, once by naphthalene (between blocks) and second by anthracene (at the end of the poly(methacrylic acid) block).[48] In pure water, we have obtained for the hydrodynamic radius, R_H, ca. 30 nm and the micellar molar mass, $(M_w)_M$ ca. 8.0×10^6 g mol^{-1}. The radius of the core, R_C, was

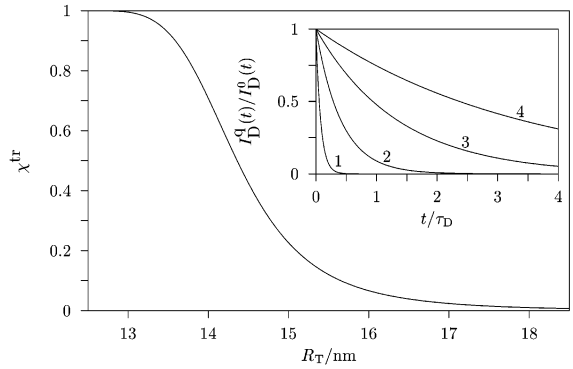

Figure 1. Dependence of the transfer efficiency, χ^{tr}, on R_T for the "simplistic" model of a uniform micelle with $R_C = 12.5$ nm, $R_0 = 2.1$ nm, and $N_T = 200$ (see eq 5). Inset: Time-resolved donor emissions $I_D{}^q(t)/I_D{}^0$ (t) for $R_T = 13.5$ nm (curve 1), $R_T = 14.0$ nm (2), $R_T = 14.5$ nm (3), and $R_T = 15.0$ nm (4). Note that all these decays are exponential.

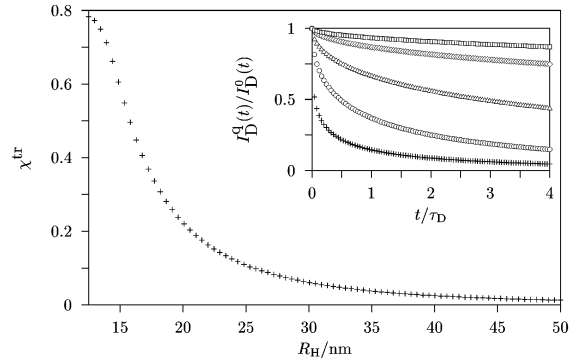

Figure 2. Transfer efficiency, χ^{tr}, as a function of R_H for the 3D random model (uniformangular and random radial distribution of traps in the shell) with $R_C = 12.5$ nm, $R_0 = 2.1$ nm, and $N_T = 200$. Inset: Time-resolved donor emissions $I_D{}^q(t)/I_D{}^0$ (t) for $R_H = 12.5$ nm (+), $R_H = 15.4$ nm (○), $R_H = 18.5$ nm (△), $R_H = 24.5$ nm (◇), and $R_H = 30.5$ nm (□). The error bars are not shown, because they are negligible.

calculated from the $(M_w)_M$ value and the copolymer composition assuming the core density 1.05 g cm^{-3}, which is the density of the glassy polystyrene.[69,76] The calculated radius, R_C ca. 12.5 nm, is close to the experimental value obtained by small-angle neutron scattering for polystyrene-poly(methacrylic acid) micelles formed by a copolymer with a very similar length of blocks.[77] Since the association number is close to 200, we assume, for simplicity, that one micelle is formed by 200 of copolymer chains. For the Förster radius, we use, $R_0 = 2.1$ nm which was reported in the literature for the naphthalene-to-anthracene energy transfer in a nonpolar medium.[71,78]

Figure 1 shows the transfer efficiency, χ^{tr}, calculated for the "simplistic" model, i.e., from eq 5, as a function of R_T (note that the donor−trap separation is $R_T - R_C$). The shape of χ^{tr} vs R_T is basically similar to that of an isolated donor−trap pair. The sigmoidal drop is not fully symmetrical and the 50% transfer efficiency is reached at appreciably smaller R_T than $R_C + R_0$ (at $R_T = R_C + R_0$, the efficiency is only ca. 30%). The insert in Figure 1 shows the ratio $I_D{}^q(t)/I^0{}_D(t)$ for several R_T values, calculated using $(k_{tr})_{mean}$ from eq 4.

Transfer efficiency, χ^{tr}, for the "3D random" distribution of traps is shown in Figure 2, together with the donor fluorescence decays, $I_D{}^q(t)/I^0{}_D(t)$ in the inset. Numerical results were obtained by Monte Carlo simulations using eqs 8 and 9. Each value represents the

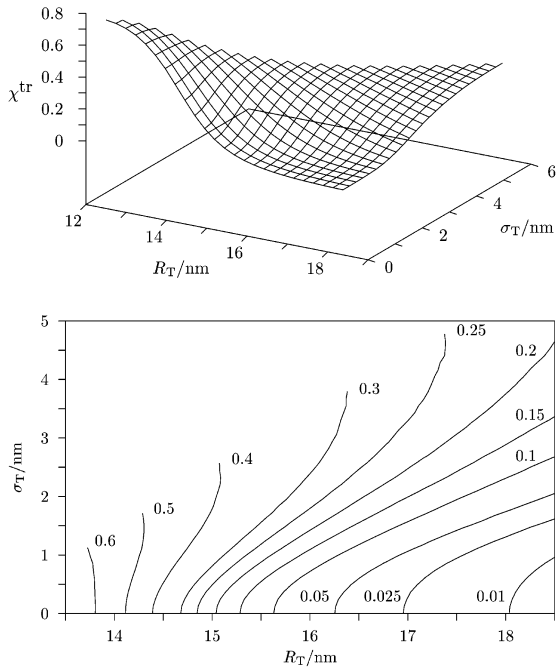

Figure 3. Transfer efficiency, χ^{tr}, as a function of R_T and σ_T for the Gaussian radial distribution of traps in the shell with $R_C = 12.5$ nm, $R_0 = 2.1$ nm, and $N_T = 200$. The contour diagram, i.e., the map of curves for constant transfer efficiencies, is shown at the bottom.

ensemble average of 4×10^5 configurations. The minimum donor−trap distance, which controls the transfer rate to a great extent, is small in some micelles, but it can be fairly large in the others. Therefore, energy transfer is important for a relatively small fraction of micelles, while the remaining fraction of micelles are unaffected by NRET. The NRET efficiency and nonexponential shapes of $I_D{}^q(t)/I_D{}^0(t)$ depend strongly on R_H.

The results of simulations for the Gaussian distribution are shown in Figures 3 and 4. Figure 3 shows the transfer efficiency, χ^{tr}, as a function of $R_T = R_C + R^{ef}$ and σ_T. As expected, the same χ^{tr} values are obtained for a number of different R_T and σ_T. The map of "isoefficiency" curves for constant χ^{tr} values is depicted below the χ^{tr} surface in the (R_T, σ_T) plane. However, systems with the same χ^{tr} and different combinations of R_T and σ_T may be distinguished by the time-resolved fluorescence decays. In Figure 4a, five representative $I_D{}^q(t)/I_D{}^0(t)$ curves for $\chi^{tr} = 0.1$ but different R_T and σ_T values are shown, and for $\chi^{tr} = 0.3$, they are shown in Figure 4b. The curves for small σ_T and corresponding small R_T are only slighly curved as compared with those for larger σ_T and R_T. The differences between individual curves are more pronounced in the case of a low transfer efficiency.

The results of simulations using the Gaussian model for $\sigma_T = 0$ are summarized in Figure 5. It is evident that the angular fluctuations of trap positions leads to the fluorescence behavior that differs from the simplistic "uniform micelle" model. Despite the fact that all traps are in the same distance from the core/shell interface their angular fluctuations with respect to the donor results in nonexponential fluorescence decay curves. This is expected from the BF calculation for small d (cf. eqs 6 and 7).

Figure 6 shows results for the Maxwellian radial distribution of traps in the shell. The decays resemble those obtained for the Gaussian distribution, but the

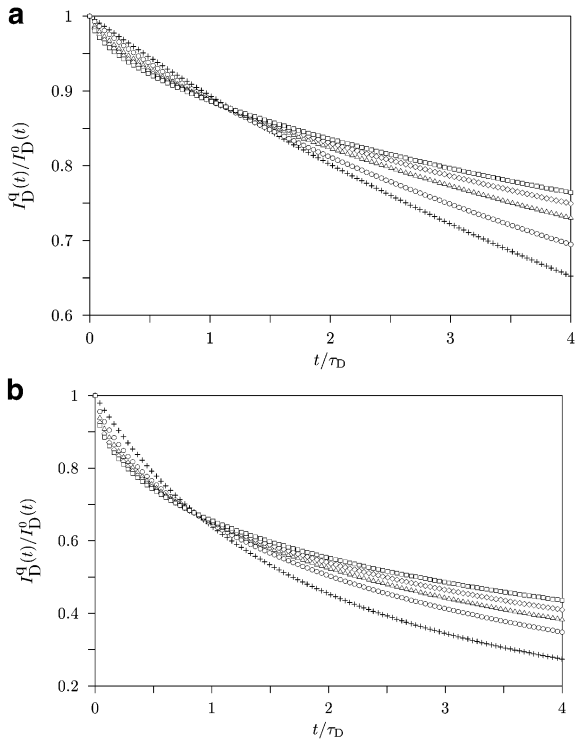

Figure 4. (a) Gaussian distribution of traps. The time-resolved donor emissions $I_D{}^q(t)/I_D{}^0$ (t) for five selected combinations of R_T and σ_T, all corresponding to $\chi^{tr} = 0.1$ for $R_T = 15.63$ nm, $\sigma_T = 0.00$ nm (+), $R_T = 16.30$ nm, $\sigma_T = 1.00$ nm (○), $R_T = 17.03$ nm, $\sigma_T = 1.59$ nm (△), $R_T = 17.69$ nm, $\sigma_T = 2.08$ nm (◇), and $R_T = 18.50$ nm, $\sigma_T = 2.68$ nm (□). (b) Analogous curves for $\chi^{tr} = 0.3$ as in Figure 4a for $R_T = 14.68$ nm, $\sigma_T = 0.00$ nm (+), $R_T = 15.03$ nm, $\sigma_T = 0.86$ nm (○), $R_T = 15.32$ nm, $\sigma_T = 1.29$ nm (△), $R_T = 15.68$ nm, $\sigma_T = 1.84$ nm (◇), and $R_T = 16.38$ nm, $\sigma_T = 3.80$ nm (□).

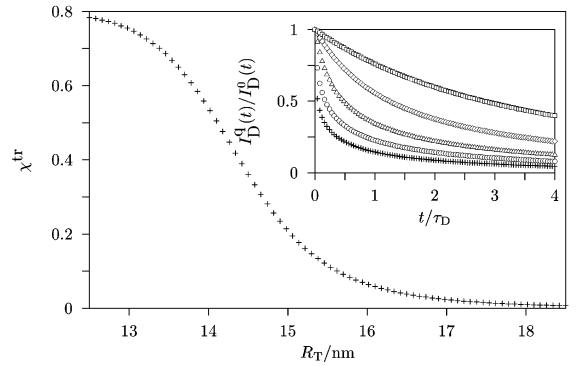

Figure 5. Transfer efficiency, χ^{tr}, as a function of R_T for the random angular and the Gaussian radial distribution with $\sigma_T = 0$ (this mimics the "simplistic" model) for $R_C = 12.5$ nm, $R_0 = 2.1$ nm, and $N_T = 200$. Inset: Time-resolved donor emissions, $I_D{}^q(t)/I_D{}^0$ (t) for $R_T = 12.5$ nm (+), $R_T = 13.5$ nm (○), $R_T = 14.0$ nm (△), $R_T = 14.5$ nm (◇), and $R_T = 15.0$ nm (□). The error bars are not shown, because they are negligible.

initial decay is generally faster. The fast initial donor fluorescence decay combined with the almost unaffected decay at later times is a typical behavior of real micellar systems in aqueous mixed solvents.[48] On the other hand faster and almost single-exponential decay was observed in the 1,4-dioxane−methanol mixed solvent.[76] The peculiar shape of experimental decay curves in aqueous media may be explained by a strongly nonuniform distribution function with a significant probability of fluctuating trap positions in a small distance of the core/shell interface and a high fraction of distant traps. The

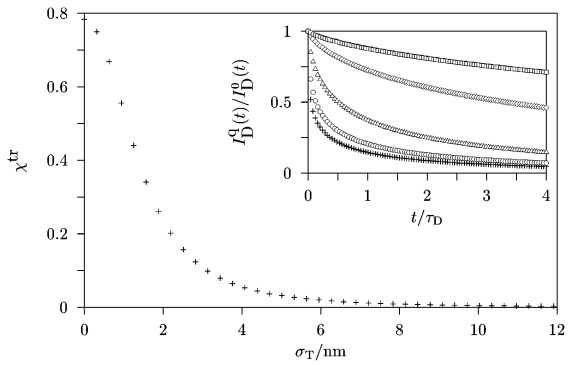

Figure 6. Transfer efficiency, χ^{tr}, as a function of σ for the random angular and the Maxwellian radial distribution of traps for $R_C = 12.5$ nm, $R_0 = 2.1$ nm, and $N_T = 200$. Inset: time-resolved donor emission $I_D{}^q(t)/I_D{}^0$ (t) for $\sigma = 0.0$ (+), 0.5 (○), 1.0 (△), 2.0 (◇), and 3.0 nm (□). The error bars are not shown, because they are negligible.

distribution function of the Maxwellian type with the maximum probability of trap locations fairly close to the core/shell interface and a relatively slowly decaying tail toward long distances may explain semiquantitatively the observed fluorescence behavior. It is worth mentioning that bimodal distributions of periphery block segments and chain ends were predicted by theoreticians on the basis of mean field calculations in copolymer brushes under certain conditions.[80] These brush systems are in many respects similar to that studied in this paper.

We believe that the Monte Carlo simulations presented herein demonstrate that the measurement of both the donor steady-state spectra and time-resolved fluorescence decays is necessary for the determination of the distribution function of the end-attached traps in micellar shells in the double-tagged polymeric micelles. This is probably the case for all studies in which fluorescence is used to extract geometric information.

Comparison of Experimental and Simulated Model Decays. In this part, we compare results of Monte Carlo simulations for a given (experimentally assessed) energy transfer efficiency with experimental decays for PS−N-PMA-A micelles in 1,4-dioxane−methanol mixtures[79] and in 1,4-dioxane−water mixtures.[48] Figure 7a shows a comparison of fluorescence decays for different 1,4-dioxane−methanol (70 vol %) mixtures. This mixture is a strongly selective precipitant for polystyrene and a marginal solvent for the anthracene tags due to its high polarity, even though pure methanol dissolves free anthracene at low concentrations. Because methanol is much less hydrophilic than water, the tendency of anthracene tags to avoid the bulk solvent is diminished. Consequently, the anthracene traps do not come close to the naphthalene donors, and the energy transfer effect is much less pronounced as compared with aqueous solvents. The experimental decay is compared with model curves for the models discussed previously, using parameters that yield the experimentally observed energy transfer efficiency. Although the curvature due to NRET is not too pronounced, nevertheless it is evident that the decay based on the Maxwellian distribution compares best with the experimental one. Despite the fact that differences between individual curves are small, it is clear that neither the simplistic nor 3D model are able to reproduce the decay well. The average donor−trap distances based on the energy transfer efficiency for the

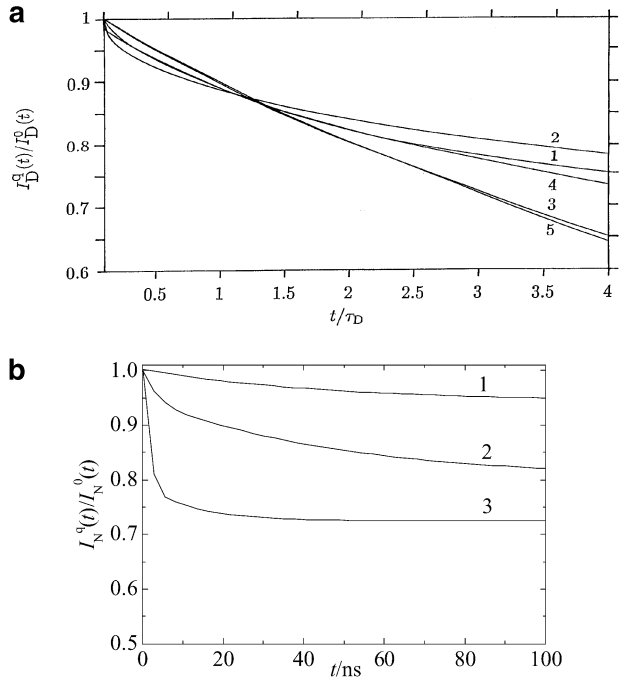

Figure 7. (a) Fitted experimental naphthalene fluorescence decay $I_D{}^q(t)/I_D{}^0(t)$ vs t/τ_D for 1,4-dioxane−methanol (70 vol %), i.e., for $\chi^{tr} = 0.1$ (curve 1) compared with simulated curves for the 3D model (curve 2), 2D model (curve 3), Maxwellian model (curve 4), and the simplistic reference model (curve 5). (b) Relative naphthalene tag fluorescence decays in solutions of polymeric samples, $I^q{}_D/I^0{}_D = f(t)$ in a 1,4-dioxane−water mixtures with 5, 20, and 100 vol % H_2O, respectively (curves 1, 2, and 3).

Gaussian and Maxwellian model distributions are similar and in the range.

Figure 7b shows decay curves for aqueous mixtures with 95 (curve 1) and 20 vol % of 1,4-dioxane (curve 2) for pure water (curve 3). In our experimental paper, we concluded that the observed curves are peculiar and that it is difficult to explain their strongly biphaseic shape by a simple single-peak radial distribution of traps in the shell. We suggested that there could be a double-peak distribution of tagged-chan conformation as has been suggested by theoreticians in some polyelectrolyte systems.[80] The comparison of the experimental curve for water with model decays in Figures 1−5 shows immediately that none of the single-peak model curves is able to reproduce the experimental decay in water-rich media (none of model decays $I_D{}^q(t)/I_D{}^0(t)$ levels off at longer times, and we did not include theoretical curves in Figure 7b). The best agreement we could get is for Maxwellian model, but the comparison is still far from being satisfactory, even at the semiquantitative level. Recently we have initiated more advanced lattice Monte Carlo simulations of hydrophobically modified shell-forming chains tethered to the hydrophobic spherical surface. Preliminary results suggest a double-peak distribution of donor−trap distances in such systems. The results of this Monte Carlo study will be published elsewhere.[81]

Despite peculiarities with the time-resolved decays, all models (except the 3D random model) suggest that the anthracene tags return fairly closely to the PS core−corona interface and the naphthalene donors. Hence, we calculated the average distance of traps from the core for micelles in 1,4-dioxane mixtures from the energy transfer efficiencies using different models. The average

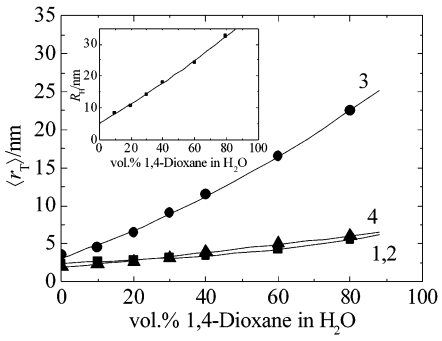

Figure 8. Average distances of anthracene traps from the core as functions of the solvent composition, evaluated from the lifetime-based values of χ^{tr} (eq 5) for the simplistic model (curve 1), 2D model (curve 2), 3D model (curve 3), and Maxwellian model (curve 4). Inset: Theoretical hydrodynamic radii of micelles, R_H, that would correspond to experimental values of χ^{tr} according to the 3D model.

linear distance of traps, $\langle r_T \rangle$, is defined by the following relation

$$\langle r_T \rangle = \int_{R_C}^{R_H} \rho_R(r) 4\pi r^2 \, dr \qquad (12)$$

where $\rho_R(r)$ is the radial distribution function of trap distances from the micelle center. For the fully random 3D-model, the linear average distance is given by the formula

$$\langle r_T \rangle = {}^3/_4 \frac{R_H{}^4 - R_C{}^4}{R_H{}^3 - R_C{}^3} \qquad (13)$$

for other models, it may also be calculated without major problems. Figure 8 shows the calculated average distances as a function of the solvent composition. Regardless of the model used (except 3D model), the curves show that anthracene-tagged ends of PMA blocks return back in the shell and come quite close to the core/shell interface. The average distances are very small in water-rich media. However, they are generally small as compared with the experimental shell thickness in the whole region of solvent compositions. The comparison shows that the fully random 3D model is incompatible not only with time-resolved, but also with the steady-state data. On one hand, the average distances $\langle r_T \rangle$ are larger than those for other models. On the other hand, the experimental values of the energy transfer efficiency would require significantly lower values of R_H than those measured in water-rich solvents and significantly higher in 1,4-dixane-rich solvents (see Figure 2 and also inset in Figure 8).

As compared with 1,4-dioxane−methanol solvents, the 3D random model proves to be even more incompatible with the experimental data for 1,4-dioxane aqueous systems We believe our experimental observations coupled with our MC simulation demonstrates the non-uniform distribution of hydrophobic traps in the corona of water-soluble PS−N-PMA-A polymeric micelles.

Summary

In this paper, we have studied the effect of hydrophobic modification of the of the ends of chains on the chain conformations that make up a polymer micelle corona. Our calculations are directed toward an interpretation of our NRET experiments in which the "hydrophobic modification" is the result of attaching a

Scheme 2. Donor-Trap Geometry for *P*(*r*) Calculation

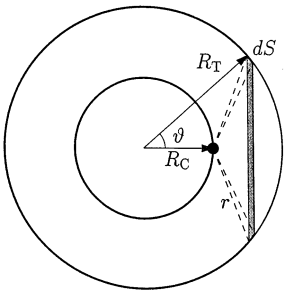

hydrophobic energy trap (anthracene) to the corona chain ends. However, other workers are considering adding "recognition elements" to the ends of the corona of polymer micelles for the purpose of directed drug delivery. In the case that the recognition elements have some degree of hydrophobic character, the considerations presented here may be highly relevant to this important application.[82−84]

Our analysis of NRET from energy donors located at the core−corona interface to energy-acceptor end-tagged corona chains has demonstrated the need to carry out explicit MC simulations because the local concentration of acceptors is too high to permit the application of KB theory. In any case, we are not aware of any analytical solution using the KB approach for the physical models discussed herein. Several simple but physically realistic models for the distribution of the acceptor in the corona $\phi_A(r)$ have been presented, and the predicted time-dependent fluorescence curves ($I_D(t)/I_0(t)$) and steady-state transfer efficiency (χ_{tr}) have been discussed. In general a unique determination of $\phi_A(r)$ from fluorescence data ($I_D(t)/I_0(t)$ and χ_{tr}) is not possible because the interplay of the model parameters is so delicate. However a similar comment could be made about classical scattering techniques, whose interpretation is also highly model dependent.

Acknowledgment. This study was supported by the Grant Agency of the Czech Republic (Grant No. 203/01/0536) and by the Grant Agency of the Charles University (Grant No. 215/2000/BCh/PrF). The numerical calculations were performed by using the computer facilities of the *Computer Meta-Center (Praha-Brno-Plzeň)* of the Ministry of Education of the Czech Republic. S.E.W. would like the acknowledge the support of the Robert A. Welch Foundation (Grant F-356).

Appendix 1. Evaluation of the Normalized Number Density of Traps *P*(*r*)

An excited donor is assumed to be located in the distance R_C from the micellar center. There are N_T traps homogeneously distributed with a constant surface density $n_T = N_T/(4\pi R_T^2)$ at the concentric spherical surface of the radius R_T. Thus, the probability that the trap has distance within $\langle r, r + dr\rangle$ is expressed in the form

$$P(r)dr = \frac{n_T\, dS}{N_T} = \frac{dS}{4\pi\, R_T^2} \qquad \text{(A1)}$$

where $dS = 2\pi R_T^2 \sin\theta\, d\theta$ is the surface of the gray ring in Scheme 2. Using the differenciated form of the identity $r^2 = R_T^2 + R_C^2 - 2R_C R_T \cos\theta$, we obtain

$$P(r)\, dr = \frac{r}{2R_C R_T} dr \qquad \text{(A2)}$$

References and Notes

(1) Guillet, J. *Polymer Photophysics and Photochemistry*; Cambridge University Press: Cambridge, England, 1985.
(2) Winnik, M. A. In *Photophysical and Photochemical Tools in Polymer Science*; Winnik, M. A., Ed.; NATO ASI Series C 182, Reidel: Dordrecht, The Netherlands, 1986.
(3) Yekta, A.; Winnik, M. A. In *Solvents and Self-Organization of Polymers*; Webber, S. E., Munk, P., Tuzar, Z., Arca, A., Eds.; Kluwer: Dordrecht, The Netherlands, 1996; p 433.
(4) Demchenko, A. P. In *Topics in Fluorescence Spectroscopy*; Lakowics, J. R., Ed.; Plenum Press: New York, 1991; Vol. 3.
(5) Morawetz, H. *Science* **1988**, *240*, 172.
(6) Morawetz, H. *J. Lumin.* **1989**, *43*, 59.
(7) Nakashima, K.; Winnik, M. A.; Dai, K. H.; Kramer, E. J.; Washiyama, J. *Macromolecules* **1992**, *25*, 6866.
(8) Ni, S.; Zhank, P.; Wang, Y.; Winnik, M. A. *Macromolecules* **1994**, *27*, 5742.
(9) Rhabi, Y.; Yekta, A.; Winnik, M. A.; DeVoe, R. J.; Barrera, D. *Macromolecules* **1999**, *32*, 3241.
(10) Mendelsohn, A. S.; de la Cruz, M. O.; Torkelson, J. M. *Macromolecules* **1993**, *26*, 6789.
(11) Holden, D. A.; Guillet, J. E. *Macromolecules* **1980**, *13*, 289.
(12) Liu, G.; Guillet, J. E.; Al-Takrity, T. B.; Jenkins, A. D.; Walton, D. R. M. *Macromolecules* **1991**, *24*, 68.
(13) Major, D. M.; Torkelson, J. M.; Brearley, A. M. *Macromolecules* **1990**, *23*, 1700.
(14) Ringsdorf, H.; Simon, J.; Winnik, F. M. *Macromolecules* **1992**, *25*, 7306.
(15) Yekta, A.; Duhamel, J.; Brochard, P.; Adiwidjaja, H.; Winnik, M. A *Macromolecules* **1993**, *26*, 1829.
(16) Schillén, K.; Yekta, A.; Ni, S.; Winnik, M. A. *Macromolecules* **1998**, *31*, 210.
(17) Farinha, J. P. S.; Schillén, K.; Winnik, M. A. *J. Phys. Chem. B* **1999**, *103*, 2487.
(18) Liu, G. *J. Phys. Chem.* **1995**, *99*, 5465.
(19) Liu G.; Smith, C. K.; Hu, N.; Tao, J. *Macromolecules* **1996**, *29*, 220.
(20) Tuzar, Z.; Kratochvíl, P. In *Surface and Colloid Science*; Matievic, E., Ed.; Plenum Press: New York, 1993; Vol. 15, p 1.
(21) Wilhelm, M.; Zhao, C.-L.; Wang, Y.; Xu, R.; Winnik, M. A.; Mura, J.-L.; Riess, G.; Croucher, M. D. *Macromolecules* **1991**, *24*, 1033.
(22) Rager, T.; Meyer, W. H.; Wegner, G.; Winnik, M. A. *Macromolecules* **1997**, *30*, 4911.
(23) Astafieva, I.; Zhong, X. F.; Eisenberg, A. *Macromolecules* **1993**, *26*, 7339.
(24) Astafieva, I.; Khougaz, K.; Eisenberg, A. *Macromolecules* **1995**, *28*, 7127.
(25) Yu, Y. S.; Zhang, L. F.; Eisenberg, A. *Langmuir* **1997**, *13*, 2578.
(26) Zhang, L. F.; Eisenberg, A. *Macromolecules* **1999**, *32*, 2239.
(27) Shen, H. W.; Zhang, L. F.; Eisenberg, A. *J. Am. Chem. Soc.* **1999**, *121*, 2728.
(28) Shen, H. W.; Eisenberg, A. *J. Phys. Chem. B* **1999**, *103*, 9473.
(29) Shen, W. H.; Eisenberg, A. *Macromolecules* **2000**, *33*, 2561.
(30) Antonietti, M.; Heinz, S.; Schmidt, M.; Rosenauer, C. *Macromolecules* **1994**, *27*, 3276.
(31) Antonietti, M.; Förster, S.; Östrich, S. *Macromol. Symp.* **1997**, *121*, 75.
(32) Regenbrecht, M.; Akari, S.; Förster, S.; Mohwald, H. *J. Phys. Chem. B* **1999**, *103*, 6669.
(33) Buthun, V.; Lowe, A. B.; Billingham, N. C.; Armes, S. P. *J. Am. Chem. Soc.* **1999**, *121*, 4288.
(34) Lee, A. S.; Gast, A. P.; Buthun, V.; Armes, S. P. *Macromolecules* **1999**, *32*, 4302.
(35) Wooley, K. L. *J. Polym. Sci.* **2000**, *38*, 1397.
(36) Kiserow, D.; Procházka, K.; Ramireddy, C.; Tuzar, Z.; Munk, P.; Webber, S. E. *Macromolecules* **1992**, *25*, 461.
(37) Tian, M.; Quin, A.; Ramireddy, C.; Webber, S. E.; Munk, P.; Tuzar, Z.; Procházka, K. *Langmuir* **1993**, *9*, 1741.
(38) Teng, Y.; Morrison, M.; Munk, P.; Webber, S. E.; Procházka, K. *Macromolecules* **1998**, *31*, 3578.
(39) Štěpánek, M.; Krijtová, K.; Limpouchová, Z.; Procházka, K.; Teng, Y.; Webber, S. E.; Munk, P. *Acta Polym.* **1998**, *49*, 96; **1998**, *49*, 103.
(40) Procházka, K.; Martin, T. J.; Munk, P.; Webber, S. E. *Macromolecules* **1996**, *29*, 6518.
(41) Štěpánek, M.; Procházka, K. *Langmuir* **1999**, *15*, 8800.
(42) Štěpánek, M.; Procházka, K.; Brown, W. *Langmuir* **2000**, *16*, 2502.
(43) Procházka, K. *J. Phys. Chem.* **1995**, *99*, 14108.

(44) Viduna, D.; Limpouchová, Z.; Procházka, K. *Macromolecules* **1997**, *30*, 7263.
(45) Limpouchová, Z.; Viduna, D.; Procházka, K. *Macromolecules* **1997**, *30*, 8027.
(46) Jelínek, K.; Limpouchová, Z.; Procházka, K. *Macromol. Theory Simul.* **2000**, *9*, 703.
(47) Webber, S. E.; Munk, P.; Tuzar, Z.; Procházka, K. *CHEMTECH* **1998**, *28*, 20.
(48) Matějíček, P.; Limpouchová, Z.; Uhlík, F.; Procházka, K.; Tuzar, Z.; Webber, S. E. *Macromolecules* **2002**, *35*, 9487.
(49) van der Meer, W. B.; Coker, G.; Chen, S. S.-Y. *Resonance Energy Transfer*; Wiley-VCH: New York, 1991.
(50) Förster, T. *Z. Naturforsch.* **1949**, *4A*, 321.
(51) Förster, T. *Discuss. Faraday Soc.* **1959**, *7*, 27.
(52) Berleman, I. B. *Energy Transfer Parameters of Aromatic Compounds*; Academic Press: New York, 1973.
(53) Štěpánek, M.; Krijtová, K.; Procházka, K.; Teng, Y.; Webber, S. E. *Colloids Surf. A*, **1999**, *147*, 79.
(54) Yang, C. L.; Evesque, P.; El-Sayed, M. A. *J. Phys. Chem.* **1985**, *89*, 3442.
(55) Yang, C. L.; El-Sayed, M. A.; Suib, S. L. *J. Phys. Chem.* **1987**, *91*, 4440.
(56) Klafter, J.; Blumen, A. *J. Lumin.* **1985**, *34*, 77.
(57) Blumen, A.; Klafter, J.; Zumhofen, G. *J. Chem. Phys.* **1986**, *84*, 1397.
(58) Gochanour, C. R.; Andersen, H. C.; Fayer, M. D. *J. Chem. Phys.* **1979**, *70*, 4254.
(59) Ediger, M. D.; Fayer, M. D. *J. Chem. Phys.* **1983**, *78*, 2518.
(60) Baumann, J.; Fayer, M. D. *J. Chem. Phys.* **1986**, *85*, 4087.
(61) Ediger, M. D.; Dominique, R. P.; Fayer, M. D. *J. Chem. Phys.* **1988**, *89*, 5224.
(62) Keller, L.; Hussey, D. M.; Fayer, M. D. *J. Phys. Chem.* **1996**, *100*, 10257.
(63) Frederickson, G. H.; Andersen, H. C.; Frank, C. W. *J. Chem. Phys.* **1983**, *79*, 3572.
(64) Frederickson, G. H.; Frank, C. W. *Macromolecules* **1983**, *16*, 1198.
(65) Farinha, J. P. S.; Martinho, J. M. G.; Yekta, A.; Winnik, M. A. *Macromolecules* **1995**, *28*, 6084.
(66) Farinha, J. P. S.; Martinho, J. M. G.; Kawagushi, S.; Yekta, A.; Winnik, M. A. *J. Phys. Chem.* **1996**, *100*, 12552.
(67) Yekta, A.; Winnik, M. A.; Farinha, J. P. S.; Martinho, J. M. G. *J. Phys. Chem.* **1997**, *101*, 1787.
(68) Baumann, J.; Fayer, M. D. *J. Chem. Phys.* **1986**, *85*, 4087.
(69) Brandrup, J., Immergut, E. H., Eds.; *Polymer Handbook*, Interscience Publishers: New York, 1967.
(70) Pleštil, J.; Kříž, J.; Tuzar, Z.; Procházka, K.; Melnichenko, Yu. B.; Wignall, G. D.; Talingting, M. R.; Munk, P.; Webber, S. E. *Macromol. Chem. Phys.* **2001**, *202*, 553.
(71) Kiserow, D.; Chan, J.; Ramireddy, C.; Munk, P.; Webber, S. E. *Macromolecules* **1992**, *25*, 5338.
(72) Dan, N.; Tirrell, M. *Macromolecules* **1992**, *25*, 2890.
(73) Wijmans, C. M.; Zhulina, E. B. *Macromolecules* **1993**, *26*, 7214.
(74) Toral, R.; Chakrabarti, A. *Phys. Rev. E* **1993**, *47*, 4240.
(75) Grest, G. S.; Murat, M. In *Monte Carlo and Molecular Dynamics Simulations in Polymer Science*; Binder, K., Ed.; Oxford University Press: New York, 1995; p 476.
(76) Chan, J.; Fox, S.; Kiserow, D.; Ramireddy, C.; Munk, P.; Webber, S. E. *Macromolecules* **1993**, *26*, 7016.
(77) Martin, T. J.; Webber, S. E. *Macromolecules* **1995**, *28*, 8845.
(78) Berlman, I. B. *Energy Transfer Parameters of Aromatic Compounds*; Academic Press: New York, 1973.
(79) Matějíček, P.; Uhlík, F.; Limpouchová, Z.; Procházka, K.; Tuzar, Z.; Webber, S. E. *Collec. Czech. Chem. Commun.* **2002**, *67*, 531.
(80) Susharina, N. P.; Linse, P. *Eur. Phys. J.* **2001**, E*4*, 399.
(81) Uhlík, F.; Jelínek, K.; Limpouchová, Z.; Procházka, K. *J. Chem. Phys.*, submitted.
(82) Kataoka, K.; Harashima, H. *Adv. Drug Delivery Rev.* **2001**, *52*, 151.
(83) Yamamoto, Y.; Nagasaki, Y.; Kato, Y.; Sugiyama, Y.; Kataoka, K. *J. Controlled Release* **2001**, *77*, 27.
(84) Nagasaki, Y.; Yasugi, K.; Yamamoto, Y.; Harada, A.; Kataoka, K. *Biomacromolecules* **2001**, *2*, 1067.

MA012073O